

Homoclinic orbits of invertible maps

J M Bergamin, T Bountis and M N Vrahatis

Department of Mathematics and Center for Research and Applications of Nonlinear Systems,
University of Patras, Patras 26500, Greece

E-mail: jeroen.bergamin@hotmail.com

Received 26 February 2002

Published 1 August 2002

Online at stacks.iop.org/Non/15/1603

Recommended by P Cvitanović

Abstract

In this paper, we present a systematic method for finding all homoclinic orbits of invertible maps in any finite dimension. One advantage of this method is that it can also be used to order and classify all the homoclinic orbits, using symbolic dynamics, if a certain criterion is satisfied. We also present a more direct scheme, which quickly locates homoclinic orbits without, however, being able to order and classify them. Our work represents an extension of a method introduced in an earlier paper, with which one could only find homoclinic orbits possessing a certain symmetry. Thus, asymmetric homoclinic orbits can now be as easily computed. One application of our results is the explicit construction of breather (and multibreather) solutions of a class of one-dimensional nonlinear lattices.

Mathematics Subject Classification: 37C29, 37M99

1. Introduction

The accurate computation of homoclinic (or heteroclinic) orbits of multi-dimensional maps and the study of their topological properties has long been recognized as a very important problem in nonlinear dynamical systems [1–3]. Homoclinic orbits provide an excellent means for analysing the chaotic dynamics near saddle-unstable fixed points and may be thought of as complementary to the study of regular dynamics in the vicinity of periodic orbits.

In recent years, there has been renewed interest in the computation of homoclinic orbits of multi-dimensional invertible maps as recursion relations obeyed by the Fourier coefficients of localized oscillatory modes of nonlinear lattices, or *discrete breathers* [4–10]. In the case of one-dimensional particle chains with linear nearest-neighbour coupling and quartic on-site potential, it has been demonstrated that homoclinic orbits of two-dimensional maps can provide excellent approximations, from which one can explicitly construct breathers of

arbitrary complexity [11, 12], using the rotating wave approximation. Recently, Tsironis [13] used a similar technique to derive two-dimensional maps whose homoclinic orbits can provide even better approximations to the breather solutions.

In this paper we present a systematic numerical method for computing all homoclinic orbits of invertible maps in any (finite) dimension. In a previous paper [12], Bergamin *et al* had introduced an approach (called the centre condition method (CCM)) for finding all homoclinic orbits which are symmetric (or antisymmetric) with respect to the middle particle. This paper extends that approach and introduces an explicit scheme for classifying these orbits using symbolic dynamics, when a certain criterion is satisfied. In this way, we are able to obtain highly accurate approximations of discrete breathers, even in the absence of any spatial symmetry.

Finding homoclinic orbits of maps can be done, for instance, by using shooting algorithms (see, e.g. [14, 15]) or more sophisticated methods as the one presented by Beyn and Kleinkauf [16, 17]. The latter consists of implementing a Newton–Raphson scheme to solve a system of N equations whose zeros are the homoclinic orbits. The parameter N is equal to the number of elements of an orbit. For the successful use of this algorithm, an initial condition is necessary, which is chosen arbitrarily. Our method, on the other hand, does not require an initial guess and has no convergence problems when using the Newton–Raphson scheme. It finds all homoclinic orbits (unlike most shooting methods) with an accuracy that is entirely under control.

Let us write a general, invertible map $f : \mathbb{R}^g \rightarrow \mathbb{R}^g$, $g \geq 1$ as

$$x_{n+1} = f(x_n), \quad x_n \in \mathbb{R}^g, \quad n \in \mathbb{Z}, \quad (1)$$

whose inverse is

$$x_{n-1} = f^{-1}(x_n).$$

We shall assume that the origin is an equilibrium point (i.e. $f(0) = 0$) of the saddle type and study orbits homoclinic to this equilibrium (i.e. orbits $\{x_n\}$, $n \in \mathbb{Z}$, with the property $x_n \rightarrow 0$ as $n \rightarrow \pm\infty$).

Our main approach consists of deriving a new map (a second-difference map which we shall call the *special form map* (SFM)) with dimension $4g$, whose homoclinic orbits that satisfy a simple symmetry condition yield all the homoclinic orbits of the original map. Numerically, finding these symmetric homoclinic orbits of the SFM becomes a search for zeros of a nonlinear system of equations in a restricted domain of a g - or $2g$ -dimensional space, depending on the complexity of the problem. Using then a topological degree method [23–26], we are able to find all zeros and thus all homoclinic orbits of the original map.

Employing symbolic dynamics to describe the properties of maps is a common practice, adopted by many authors in the literature [18–22]. Using the symmetry of the homoclinic orbits of the SFM, our method provides a way of partitioning phase space in a natural way and then employs a symbolic representation to identify the different homoclinic orbits.

At the end of our paper, we also discuss a more direct method for computing homoclinic orbits which begins by writing (1) as a map of dimension $2g$. The homoclinic orbits of this map correspond directly to the homoclinic orbits of the original map. We again derive a system of g equations with g unknowns whose zeros correspond to the homoclinic orbits. However, there is no symmetry present in this case and thus we are not able to identify each homoclinic orbit with a symbolic sequence, as we did with our first method. If one is only interested in getting homoclinic orbits, this more direct approach is perfectly suited for it.

To present our main method, we first construct the SFM in section 2 and describe in section 3 the ideas of symbolic dynamics used to classify our solutions. Then, in section 4 we

illustrate this method by applying it to the cubic map

$$x_{n+1} + x_{n-1} = 3x_n^3 - Cx_n, \quad x_n \in \mathbb{R}. \tag{2}$$

Homoclinic orbits of this two-dimensional example approximate very accurately spatially localized, time-periodic solutions (i.e. discrete breathers) of the form $u_n(t) \approx 2\sqrt{\alpha}x_n \cos(\omega t)$, with $C = -(2 + (K - \omega^2)/\alpha)$, where $u_n(t)$ satisfies the differential-difference equation

$$\ddot{u}_n + Ku_n + u_n^3 - \alpha(u_{n+1} - 2u_n + u_{n-1}) = 0$$

(see [11] for more details).

In section 5 we present our second more direct method and apply it to find homoclinic orbits of the famous Hénon map [27]

$$\begin{aligned} x_{n+1} &= 1 + by_n - ax_n^2, \\ y_{n+1} &= x_n, \end{aligned} \quad x_n, y_n \in \mathbb{R}. \tag{3}$$

Finally, in section 6 we describe how these methods may be used to find *heteroclinic* orbits in invertible maps and end with some concluding remarks.

2. Construction of the SFM

In order to apply our method, we first need to rewrite the map (1) as follows:

$$X_{n+1} + MX_{n-1} = F(X_n), \quad X_n \in \mathbb{R}^d, \tag{4}$$

where M is a $d \times d$ matrix which can have two forms: when $d = 1$ we take $M = 1$; when $d > 1$ we require that d be even and write

$$M = \begin{pmatrix} Id_g & 0 \\ 0 & -Id_g \end{pmatrix}, \quad g = \frac{d}{2},$$

with the obvious property $M = M^{-1}$ (Id_g denotes the $g \times g$ identity matrix). We still demand, of course, that $F(0) = 0$ be a saddle equilibrium, which possesses homoclinic orbits. Note that (1) can always be written in the form (4) by defining

$$X_n = \begin{pmatrix} x_n \\ y_n \end{pmatrix} \in \mathbb{R}^d, \quad d = 2g,$$

so that

$$X_{n+1} + MX_{n-1} = \begin{pmatrix} f(x_n) + f^{-1}(x_n) \\ f(y_n) - f^{-1}(y_n) \end{pmatrix} \equiv F(X_n).$$

Homoclinic orbits of (5) are homoclinic orbits of (1) under the condition $x_n = y_n$ for all n . This condition will reduce the dimension of the space in which we search for homoclinic orbits, as will be explained later on (see the text following equation (12)).

We now introduce what we shall call the SFM as

$$A_{n+1} + KA_{n-1} = L\hat{G}(A_n), \tag{5}$$

where

$$A_n = \begin{pmatrix} V_n \\ W_n \end{pmatrix} \in \mathbb{R}^{2d},$$

with $V_n, W_n \in \mathbb{R}^d$,

$$K = \begin{pmatrix} M & 0 \\ 0 & M \end{pmatrix}, \quad L = \begin{pmatrix} Id_d & M \\ Id_d & -M \end{pmatrix}$$

and

$$\hat{G}(A_n) = \begin{pmatrix} F\left(\frac{V_n + W_n}{2}\right) \\ F\left(\frac{V_n - W_n}{2}\right) \end{pmatrix}.$$

If we define

$$V_n = X_n + X_{-n}, \quad (6a)$$

$$W_n = X_n - X_{-n}, \quad (6b)$$

it is easy to show that all homoclinic orbits of (4) correspond to homoclinic orbits of the SFM (5) obeying the symmetry condition

$$A_n = S_d A_{-n}, \quad \forall n, \quad (7)$$

with

$$S_d = \begin{pmatrix} Id_d & 0 \\ 0 & -Id_d \end{pmatrix}$$

and vice versa. Indeed, if X_n is an orbit of (4), it is clear from (6a) and (6b) that systems (4) and (5) are compatible. Thus, if X_n is a homoclinic orbit (i.e. $X_n \rightarrow 0$ as $n \rightarrow \pm\infty$), so is A_n . On the other hand, if A_n is a homoclinic orbit of the SFM (5) (i.e. $V_n \rightarrow 0, W_n \rightarrow 0$ as $n \rightarrow \pm\infty$), then by virtue of (6a) and (6b) so is the corresponding X_n .

According to this observation, locating the homoclinic orbits of (4) can be achieved by finding all homoclinic orbits of the SFM obeying symmetry property (7). To check if an orbit of (5) has the required symmetry, it is only necessary to verify it at the points $n = 0$ and $n = 1$ (see appendix A for a proof), i.e.

$$A_1 = S_d A_{-1}, \quad A_0 = S_d A_0.$$

For $d = 1$ this reduces (after using the map (5) with $n = 0$) to the condition

$$V_1 - V_{-1} = 0, \quad W_0 = 0, \quad (8)$$

while for $d > 1$ and even, it becomes

$$V_1^{(1)} - V_{-1}^{(1)} = 0, \quad W_1^{(2)} + W_{-1}^{(2)} = 0, \quad W_0^{(1)} = 0, \quad W_0^{(2)} = 0, \quad (9)$$

where the superscripts denote the first $d/2$ components and the last $d/2$ components of the vectors V_n and W_n . Thus, both (8) and (9) represent a system of $2d$ equations, satisfied by all orbits of (5) which obey the symmetry condition (7).

The problem is, therefore, reduced to a search for the roots of this system of equations. To guarantee that we find all the zeros (and thus all the homoclinic orbits), we use the notion of the topological degree. This convenient method of finding all the zeros of a system of equations in any (finite) dimension has been discussed in detail in [23–26]. For completeness, we describe its main steps here in appendix B.

Let us now define in which space we search for zeros. Clearly, we need the values of A_{-1} , A_0 and A_1 for each possible orbit of (5) to check whether (8) or (9) is fulfilled. To obtain A_{-1} , A_0 and A_1 , we first define

$$B_n = \begin{pmatrix} A_n \\ A_{n-1} \end{pmatrix},$$

such that we have a new $4d$ map

$$B_{n+1} = \begin{pmatrix} L\hat{G}(A_n) - K A_{n-1} \\ A_n \end{pmatrix} \quad (10)$$

and choose B_{-N} with $N \gg 1$ such that $B_{-N-n} \rightarrow 0$ as $n \rightarrow \infty$ (i.e. B_{-N} is on the unstable manifold of the equilibrium at the origin). We then apply the map (10) $N + 1$ times, to obtain B_0 and B_1 , and hence A_{-1} , A_0 and A_1 . Since the unstable manifold of the origin has dimension $2d$, we can determine B_{-N} by a $2d$ -dimensional coordinate on this manifold, which we shall call σ .

One straightforward way to choose B_{-N} is to take its projection on the unstable eigenspace spanned by the eigenvectors of the equilibrium whose eigenvalues have absolute value larger than 1, placing it very close to the origin, i.e.

$$B_{-N} = \epsilon \sum_{i=1}^{2d} \sigma_i E_i, \tag{11}$$

with

$$J E_i = \lambda_i E_i, \tag{12}$$

where J is the Jacobian matrix of the system (10) at the origin and $|\lambda_i| > 1$ are associated eigenvalues. The parameter $0 < \epsilon \ll 1$ is an accuracy parameter.

The vector σ is indeed sufficient for determining the entire orbit. Thus, we will now search for roots in σ -space of the system (8) or (9) with V_n and W_n being functions of σ with N and ϵ as parameters. This gives $2d$ equations which must be solved for $2d$ unknowns (the components of σ). Notice that the restriction imposed by the condition mentioned below equation (5) will yield only d equations but will also have only d unknowns.

If ϵ is taken small enough (i.e. the linear eigenspace is a good approximation of the nonlinear unstable manifold), the behaviour of the map is approximately determined by its linear part and we can write

$$B_{-N-1} = \epsilon \sum_{i=1}^{2d} \frac{\sigma_i}{\lambda_i} E_i = \epsilon \sum_{i=1}^{2d} \sigma'_i E_i, \tag{13}$$

such that increasing N by 1 is approximately equivalent to dividing all σ_i s by their respective λ_i s. Therefore, the domain in σ -space in which we search for zeros can be restricted, for example, by

$$-\lambda_i^2 \leq \sigma_i \leq \lambda_i^2, \quad \forall i. \tag{14}$$

The zeros outside this domain can be brought into this domain in groups, by increasing N (since $|\lambda_i| > 1$ we have $|\sigma'_i| < |\sigma_i|$ in (13)). Therefore, N acts as an indicator of different orbit ‘generations’. As we will see in the next section on symbolic dynamics, this role of N is directly related to the ordering of the homoclinic orbits.

3. Symbolic dynamics

Increasing N by 1 (while keeping ϵ and σ constant) simply moves all particles by one position. The new orbit, in general, will not obey any symmetry. Thus, since we want it to obey symmetry condition (7), there are two quantities to be determined, namely V_0 and W_{-1} (since $W_0 \equiv 0$). The possible values for V_0 and W_{-1} depend on the form of the map itself. This introduces a *symbolic naming* by which each of the possible values is assigned a symbol uniquely identifying each orbit. After the method has been presented, a condition is given which must be fulfilled for the method to be applied. Let us now return to the concept of the SFM and explain all this in detail for the case where $d = 1$. The case $d > 1$ and even can be treated in the same way.

Observe first that equation (5) can be written as two coupled maps, one for V_n and one for W_n :

$$\begin{aligned} V_{n+1} + MV_{n-1} &= F\left(\frac{V_n + W_n}{2}\right) + MF\left(\frac{V_n - W_n}{2}\right), \\ W_{n+1} + MW_{n-1} &= F\left(\frac{V_n + W_n}{2}\right) - MF\left(\frac{V_n - W_n}{2}\right). \end{aligned} \quad (15)$$

All the orbits we are looking for have the required symmetry (7) and hence they satisfy

$$V_1 = V_{-1}, \quad W_0 = 0,$$

which gives, for $n = 0$ in the first equation of (15) and $n = -1$ in the second,

$$V_{-1} = F\left(\frac{V_0}{2}\right), \quad MW_{-2} = F\left(\frac{V_{-1} + W_{-1}}{2}\right) - MF\left(\frac{V_{-1} - W_{-1}}{2}\right). \quad (16)$$

Consider now the following transformation, mapping a complete (known) orbit onto another, indicated here by primes:

$$\begin{aligned} V'_{\pm(n+1)} &= V_{\pm n}, & \forall n \geq 0, \\ W'_{\pm(n+1)} &= W_{\pm n}, & \forall n > 0, \\ W'_0 &= 0. \end{aligned} \quad (17)$$

This transformation does not specify V'_0 , W'_{-1} and W'_1 . Thus, we impose the symmetry (7) on the orbit denoted by the prime (so that $W'_1 = -W'_{-1}$) and assume that the original orbit also obeys the symmetry.

We also impose the map equations on the orbit denoted by the prime, so that its system of equations takes the same form as (16) with all variables primed. Upon using (17), this yields

$$V_0 = F\left(\frac{V'_0}{2}\right), \quad MW_{-1} = F\left(\frac{V_0 + W'_{-1}}{2}\right) - MF\left(\frac{V_0 - W'_{-1}}{2}\right), \quad (18)$$

which are two equations with two unknowns (V'_0 and W'_{-1}). We consider this as a map $H : (V'_0, W'_{-1}) \rightarrow (V_0, W_{-1})$. Notice, however, that this map is in the wrong direction: from the orbit denoted by the primes we find the original (known) orbit. The interesting transformation for us, of course, is H^{-1} . However, this is not well defined since there is no unique solution. In general, there are different branches of solutions, for V'_0 and (separately) for W'_{-1} . The number of branches of one unknown might depend on the value of the other unknown. However, the maximum number of possible branches is fixed.

Suppose that there is a maximum of k_1 branches of solutions V'_0 and a maximum of k_2 branches of solutions W'_{-1} . To each of the k_1 and k_2 branches, we assign a different symbol. Then, any solution of (18) can be indicated by two symbols: one for the V'_0 -branch and one for the W'_{-1} -branch.

Let us consider the transformation $H^{-1} : (V_0, W_{-1}) \rightarrow (V'_0, W'_{-1})$ which constitutes together with (17) a complete map. We call this map the *homoclinic orbit map* HOM since it maps a homoclinic orbit onto several others. All the new orbits are uniquely identified by the above two symbols. Thus, we are able to name all homoclinic orbits, by combining the new symbols with the symbolic name of the original homoclinic orbit to which the HOM was applied.

Let us observe that primes denote a new orbit 'generation', whose appearance through (17) is equivalent to increasing N by one in the numerical method. Thus, we may regard N as a 'generation' parameter, which also acts as an ordering parameter. In this way, using our numerical method together with the symbolic naming and ordering procedure described above, we should be able to find name and order all homoclinic orbits of any invertible map.

One important observation we wish to make here is that the HOM by itself (without using its numerical counterpart) does *not* generate true homoclinic orbits. Solutions, in general, do not obey the mapping equations (16) (with primes) at $n = -2, -1, 0, 1, 2$, even though in the *symbolic sense* they are equivalent to the real homoclinic orbits. So, the correct interpretation of the homoclinic orbit map is the following.

Suppose we have found a homoclinic orbit H_0 , for a certain N , ϵ and σ , and increase N by 1 (not changing ϵ). We then find at most $k_1 \times k_2$ homoclinic orbits with coordinates close to σ . Each of these solutions can be identified with one of the $k_1 \times k_2$ solutions of the homoclinic orbit map applied to H_0 , each one uniquely identified by two symbols. We then assign symbolic names to the new homoclinic orbits by combining the new symbols with the symbolic name of the original ('parent') orbit H_0 . This way, all homoclinic orbits are uniquely named and ordered. The example presented in the next section illustrates this procedure in detail.

The success of the above approach clearly requires that the HOM can be applied to H_0 (i.e. yields admissible results). This is only the case when V_0 and W_{-1} are in the domain of the HOM equations (18) (one can see that this is necessary since the HOM is only inversely defined and hence there might be no solutions). Therefore, the relevant criterion enabling the HOM to name homoclinic orbits is that the 'reachable range' of the HOM equations (i.e. the values V_0 and W_{-1} of all homoclinic orbits to which the HOM is applied) lie within the domain of these equations.

4. The cubic map

To illustrate our method, let us apply it to the example of a cubic map, given by

$$x_{n+1} + x_{n-1} = 3x_n^3 - Cx_n, \quad x_n \in \mathbb{R}. \quad (19)$$

As mentioned in the introduction, homoclinic orbits of this map approximately represent spatially localized, time-periodic solutions (i.e. discrete breathers) of a one-dimensional chain of linearly coupled particles with a quartic on-site potential. In earlier publications [11, 12] we were able to accurately approximate all *symmetric* (or anti-symmetric) homoclinic orbits and use these as approximations to symmetric or anti-symmetric discrete breather solutions. Here, we will apply the new method introduced in this paper to also find all the *asymmetric* homoclinic orbits which are thus approximations to asymmetric breathers.

4.1. Deriving the SFM and finding the homoclinic orbits

To derive the SFM we observe that the map (20) can be cast into the form (4) with

$$X_n = x_n, \quad M = 1, \quad F(X_n) = 3X_n^3 - CX_n,$$

while the SFM equations yield

$$\begin{aligned} V_{n+1} + V_{n-1} &= F\left(\frac{V_n + W_n}{2}\right) + F\left(\frac{V_n - W_n}{2}\right), \\ W_{n+1} + W_{n-1} &= F\left(\frac{V_n + W_n}{2}\right) - F\left(\frac{V_n - W_n}{2}\right), \end{aligned} \quad (20)$$

with $F(X_n)$ as given above. This is a four-dimensional map which we write in the form (10) with the aid of the vector $B_n = (V_n, W_n, V_{n-1}, W_{n-1})^T$.

When linearized about the fixed point at the origin, this map possesses two eigenvectors with eigenvalue $\lambda = (-C - \sqrt{C^2 - 4})/2 < -1$ for $C > 2$, which span a two-dimensional-space tangent to the unstable manifold at the origin and may be written in the form

$$E_1 = \begin{pmatrix} \lambda \\ 0 \\ 1 \\ 0 \end{pmatrix}, \quad E_2 = \begin{pmatrix} 0 \\ \lambda \\ 0 \\ 1 \end{pmatrix}.$$

Thus, we can now define

$$B_{-N} = \epsilon(\sigma_1 E_1 + \sigma_2 E_2) \tag{21}$$

as the starting point for a search for orbits satisfying the symmetry condition (7).

In figure 1 we plot the nullclines of the two components of system (8) for the above example. Intersection points of these lines are homoclinic orbits. The scaling procedure from equation (13), showing that all homoclinic orbits can be found using this method, is clearly visible.

We now use topological degree methods [23–26] to calculate the total number of zeros for different values of N (as explained appendix B) and then apply a bisection technique to locate all zeros and hence find all homoclinic orbits for each generation. For example, for $C = 8$, $N = 15$ and $\epsilon = 0.7 \times 10^{-10}$ we have located 224 homoclinic orbits in the domain given by (14), some of which are shown in figure 4. Among these orbits, of course, there are several ones which are asymmetric with respect to $n = 0$.

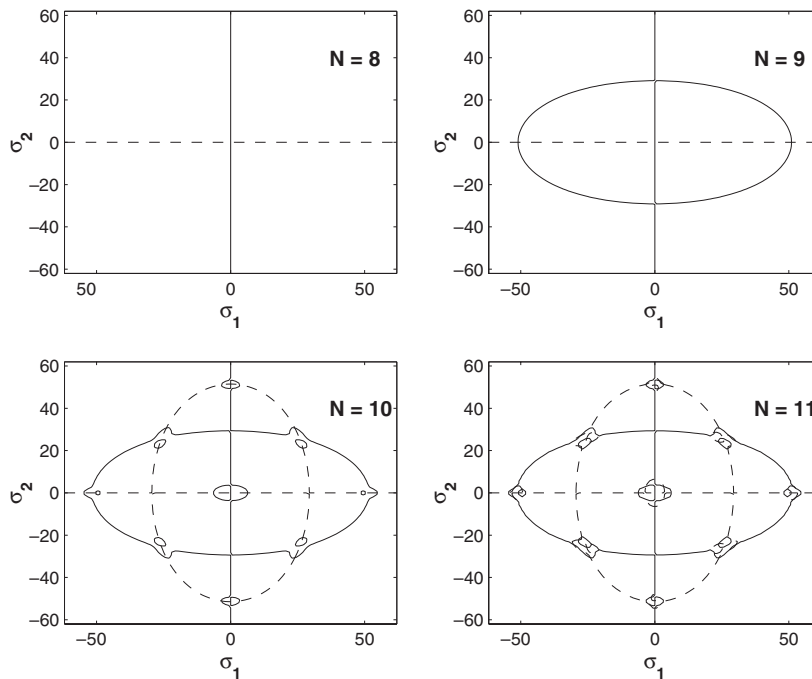


Figure 1. Nullclines of the functions $V_{-1} - V_1 = 0$ (—) and $W_0 = 0$ (---) for the map (19). Intersection points of the lines correspond to homoclinic orbits, with starting point (21) and $\sigma = (\sigma_1, \sigma_2)$. We have parameters $C = 8$, $\epsilon = 0.7 \times 10^{-10}$ and show the region (14).

4.2. Ordering and identifying the homoclinic orbits

The HOM is easily derived for this example by inserting $n = 0$ into the map equation for V_n and $n = -1$ into the map equation for W_n , setting $V_n = V'_n$, $W_n = W'_n$ and identifying V'_{-1} and W'_{-2} with V_0 and W_{-1} , respectively, to obtain

$$V_0 = F\left(\frac{V'_0}{2}\right), \quad W_{-1} = F\left(\frac{V_0 + W'_{-1}}{2}\right) - F\left(\frac{V_0 - W'_{-1}}{2}\right), \quad (22)$$

with $F(X) = 3X^3 - CX$. As explained in section 3, system (22) should be read in its inverse form, i.e. V_0 and W_{-1} are mapped onto V'_0 and W'_{-1} .

The first equation (for V'_0) can be explicitly solved. For simplicity we plot the result in the graph of figure 2. There are three branches of solutions, to which we give the symbols +, 0 and - as indicated in figure 2. The second equation (for W'_{-1}) can also be explicitly solved, but the number of branches depends on the value of V_0 . The maximum number of branches, however, is also equal to 3. We use again the symbols +, 0 and - as indicated in figure 3 for several values of V_0 and $C = 8$.

We can use the HOM to order and identify the homoclinic orbits, since the range and domain of both equations are equal to the whole real line. To show how the symbolic names are assigned, let us consider the orbit given in table 1. The symbolic name of this orbit is equal to a shifted version of the symbolic name of the orbit from which it was formed by the HOM, except for the symbols of the elements V_0 and W_{-1} , so we will only explain how to obtain these. For this, we identify the values of V_{-1} and W_{-2} with V_0 and W_{-1} and insert these in (22). We then solve for V'_0 and W'_{-1} . In table 2 we list all combinations we find and identify them with the corresponding branches of figures 2 and 3.

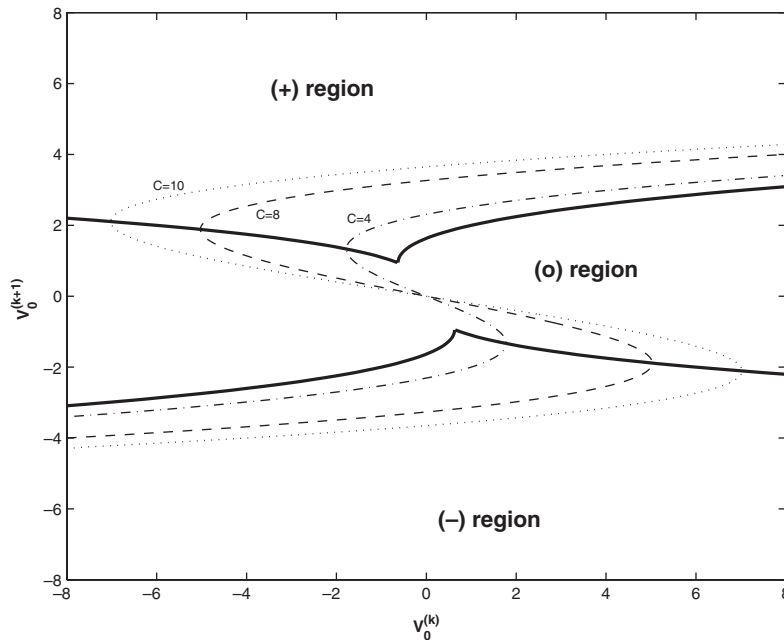


Figure 2. Partition generating the symbolic dynamics for the first component of the homoclinic orbit map (22), i.e. V_0 . The dashed, dotted and dot-dashed lines indicate the relationship between V_0 and V'_0 for various values of C . The thick, solid lines indicate the borders of the regions which have different symbols, namely (+), (0) and (-).

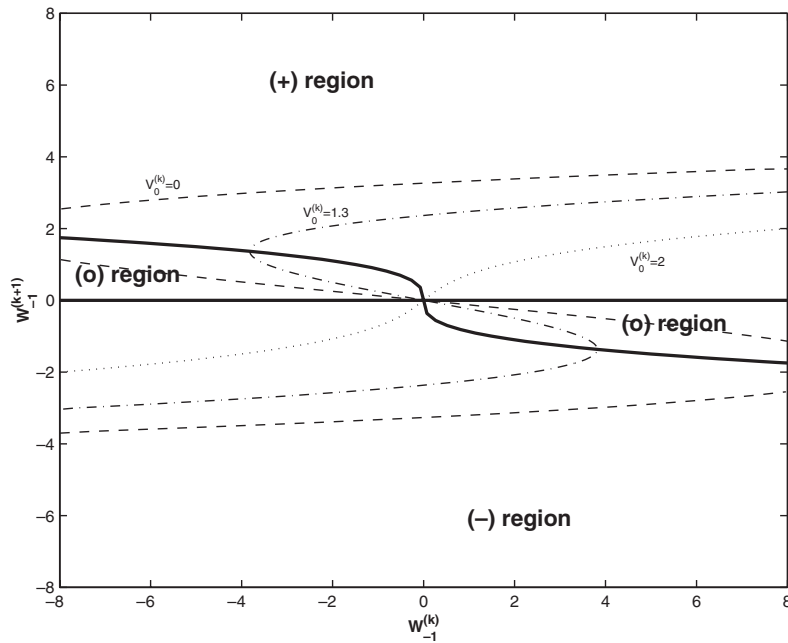


Figure 3. Partition generating the symbolic dynamics for the second component of the homoclinic orbit map (22), i.e. W_{-1} . The dashed, dotted and dot-dashed lines indicate the relationship between W_{-1} and W_{-1}^{\prime} for various values of V_0 and $C = 8$. The thick, solid lines indicate the borders of the regions which have different symbols, namely (+), (o) and (-). Observe that the (o) region becomes a single point (the origin) when $|V_0| \geq \frac{2}{3}\sqrt{C} \approx 1.89$ for $C = 8$.

Table 1. Example of a homoclinic orbit (only the central part is presented). Given here are V_n and W_n , the orbit of the SFM (20) and the resulting $X_n = (V_n + W_n)/2$ which is a homoclinic orbit of (19). See the second row, first shape in figure 4 for a graphic representation. This orbit has symbolic name (00)(-0)(00)(+-) as explained in the text.

n	V_n	W_n	X_n
-8	-0.000 014	-0.000 001	-0.000 007 5
-7	0.000 108 5	0.000 007 5	0.000 058
-6	-0.000 852	-0.000 058	-0.000 455
-5	0.006 709	0.000 457	0.003 583
-4	-0.052 82	-0.003 6	-0.028 21
-3	0.415 74	0.028 318	0.222 029
-2	-3.218 460 5	-0.211 914 5	-1.715 187 5
-1	0.002 957 5	-3.279 147 5	-1.638 095
0	3.266 356	0	1.633 178
1	0.002 957 5	3.279 147 5	1.641 052 5
2	-3.218 460 5	0.211 914 5	-1.503 273
3	0.415 74	-0.028 318	0.193 711
4	-0.052 82	0.003 6	-0.024 61
5	0.006 709	-0.000 457	0.003 126
6	-0.000 852	0.000 058	-0.000 397
7	0.000 108 5	-0.000 007 5	0.000 050 5
8	-0.000 014	0.000 001	-0.000 006 5

Table 2. All combinations (V'_0, W'_{-1}) solving the HOM (22) for the orbit with $(V_0, W_{-1}) = (V'_{-1}, W'_{-2}) = (0.002\,957\,5, -0.211\,914\,5)$, with the primed orbit given in table 1. Also shown are the symbols of the branches in figures 2 and 3 where these combinations are found. The first symbol indicates the branch of V'_0 , the second indicates W'_{-1} .

No	(V'_0, W'_{-1})	Branch symbols (VW)
1	(3.266 355 948, 3.245 295 580)	(++)
2	(3.266 355 948, 0)	(+0)
3	(3.266 355 948, -3.245 295 580)	(+-)
4	(-0.000 739 375, 3.245 295 580)	(0+)
5	(-0.000 739 375, 0)	(00)
6	(-0.000 739 375, -3.245 295 580)	(0-)
7	(-3.265 616 573, 3.245 295 580)	(-+)
8	(-3.265 616 573, 0)	(-0)
9	(-3.265 616 573, -3.245 295 580)	(--)

By comparing with the actual point $(V'_0, W'_{-1}) = (3.266\,356, -3.279\,147\,5)$, we see that the (+-) combination is closest. Since we have also found the other combinations in other orbits, we know for sure that the (+-) symbols are correct.

There is more than one way to append these new symbols to the name of the parent orbit. One can, for instance, simply add it at the end of the name. In this way, one just keeps track of the positions of V_0 and W_{-1} for each generation.

The orbit under consideration is found in the third generation of orbits starting from the trivial homoclinic orbit $A_n = 0$ for all n (zeroth generation) with symbolic name (00) (the location of both V_0 and W_{-1} is on the 0-branch). When we increase the generation by 1, all new orbits will have symbolic names (00)(vw), with (vw) the symbols identifying each orbit. Our orbit had $(vw) = (-0)$, so its symbolic name (generation 1) is (00)(-0). Its descendant we focus on has name (00)(-0)(00) (generation 2). Finally, our target orbit adds (+-) to this name as described above; so we have determined its full name to be (00)(-0)(00)(+-). Figure 4 gives several homoclinic orbits of (19) with $C = 8$ and their name according to the homoclinic orbit map. We used shortcuts to identify all nine possible combinations (vw) that occur.

5. The second method

If one is only interested in finding the homoclinic orbits of an invertible map, there is a more direct method presented in this section which gives them in a very easy way. It has many similarities with the method presented above, but does not construct symmetric orbits. This means that no ordering or explicit identifying is possible. However, the dimension of the search space will always be $2g$ and not $4g$ (g being the dimension of the original map) and this makes the method computationally more convenient.

We write the map under consideration as (1) with $x_n = X_n$ and define $Y_{n+1} = f^{-1}(Y_n)$. We see immediately that if $X_0 = Y_0$, then $Y_n = X_{-n}$ for all n . Thus, we define $A_n = (X_n, Y_n)^T$ and construct the map

$$A_{n+1} = F(A_n) \equiv \begin{pmatrix} f(X_n) \\ f^{-1}(Y_n) \end{pmatrix}. \tag{23}$$

If we now choose $A_{-N} = (X_{-N}, Y_{-N})$, $N \gg 1$, to be on the unstable manifold of (23) and apply the map N times to obtain $A_0 = (X_0, Y_0)$, we see that the identity

$$X_0 = Y_0 \tag{24}$$

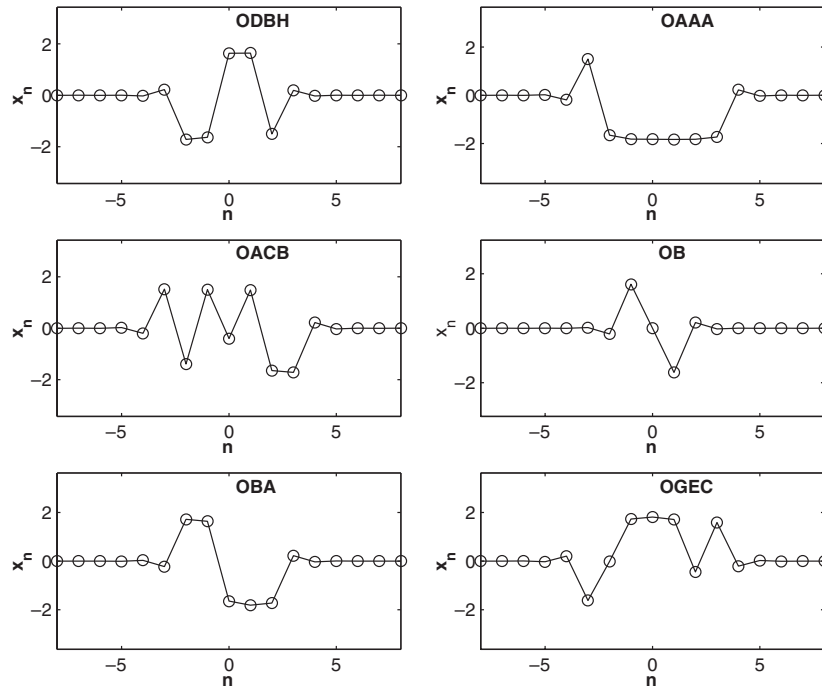


Figure 4. Several homoclinic orbits of the cubic map (19) and their symbolic name according to the HOM (22) where we used the shortcuts $A = (-+)$, $B = (0+)$, $C = (++)$, $D = (-0)$, $O = (00)$, $E = (+0)$, $F = (--)$, $G = (0-)$, $H = (+-)$.

implies $X_n = Y_{-n}$ for all n . Since $Y_{-N} \rightarrow 0$ as $N \rightarrow \infty$ (because A_{-N} is on the unstable manifold), this means that, in that limit, $X_N \rightarrow 0$ and hence A_N is on the stable manifold. Thus, we have a homoclinic orbit.

In analogy with the previous method, we approximate A_{-N} to be on the unstable manifold by choosing a point close to the origin and on the linear eigenspace of the Jacobian matrix of F at the origin (see equations (11) and (12)). This eigenspace has dimension g and hence we need a g -dimensional coordinate σ to determine the entire orbit, searching for zeros of the system of equations $X_0 - Y_0 = 0$ in this parameter space.

The lack of symmetry, however, is a significant drawback of this simple approach. First of all, it denies the possibility of assigning a symbolic name to each orbit, as was possible with the method presented in the previous sections. Second, since the eigenvalues corresponding to the eigenvectors spanning the tangent space of the unstable manifold at the origin are not equal, the location of the ‘centre’ of the homoclinic orbit (i.e. that part of the orbit where the amplitudes x_n are significantly larger than zero) is not necessarily around $n = 0$.

All this can be nicely illustrated on the example of the well-known quadratic map

$$\hat{x}_{n+1} = 1 + b\hat{y}_n - a\hat{x}_n^2, \quad \hat{y}_{n+1} = \hat{x}_n \tag{25}$$

originally due to Hénon [27].

Translating to new variables (x_n, y_n) for which the saddle equilibrium (x_{eq}, x_{eq}) of (25) ($x_{eq} = (2a)^{-1}((b - 1) + \sqrt{(b - 1)^2 + 4a})$) is at the origin, we obtain

$$x_{n+1} = 1 + by_n - a(x_n + x_{eq})^2 + (b - 1)x_{eq}, \quad y_{n+1} = x_n. \tag{26}$$

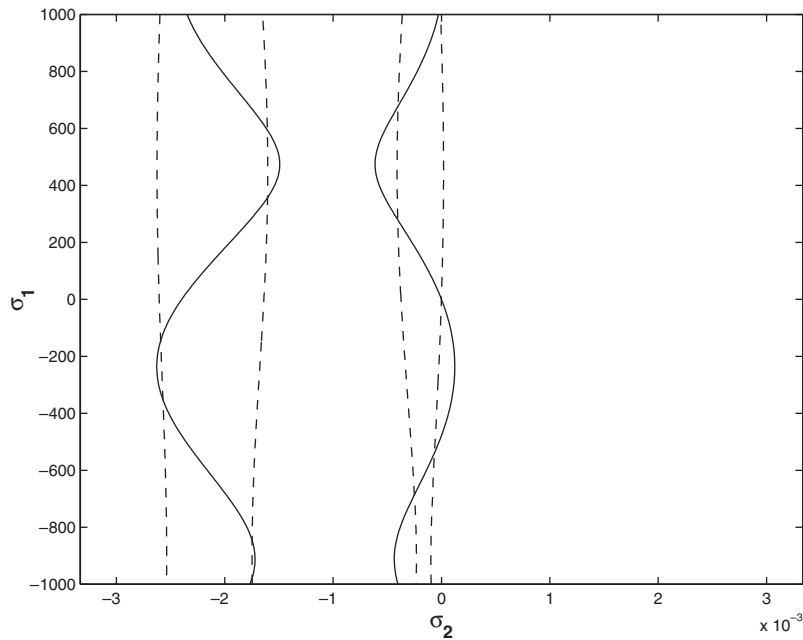


Figure 5. Nullclines of the system $x_0 - v_0 = 0$ (—) and $y_0 - w_0 = 0$ (- - -) for the map (27) at the parameter values $a = 1.4$, $b = 0.3$, $N = 8$ and $\epsilon = 1.0 \times 10^{-5}$. Notice the difference in scale for σ_1 and σ_2 which is a direct result of the inequality of the two unstable eigenvalues of the linearized map.

We then write (26) in the form (23) by setting $X_n = (x_n, y_n)$, $Y_n = (v_n, w_n)$ and $A_n = (X_n, Y_n)$ such that

$$A_{n+1} = \begin{pmatrix} f(x_n) + by_n \\ x_n \\ w_n \\ \frac{1}{b}(v_n - f(w_n)) \end{pmatrix}, \tag{27}$$

with $f(x) = 1 - a(x + x_{eq})^2 + (b - 1)x_{eq}$. Zeros of the equations

$$x_0 - v_0 = 0, \quad y_0 - w_0 = 0$$

correspond to homoclinic orbits of (26). In figure 5 these two nullclines are given. In figure 6 several homoclinic orbits of this map are presented.

Observe in figure 5 the different scale of the axes. This is a direct result of the fact that the eigenvalues of the Jacobian matrix of (27) at the origin with magnitude larger than 1 are not equal.

6. Concluding remarks

We have presented in this paper two methods for locating the homoclinic orbits of any finite dimensional, invertible map, and have successfully applied them to some typical two-dimensional examples. Although both methods use a zero-search scheme to solve systems of equations with many nearby roots, if the dimensionality of the system is not too high the

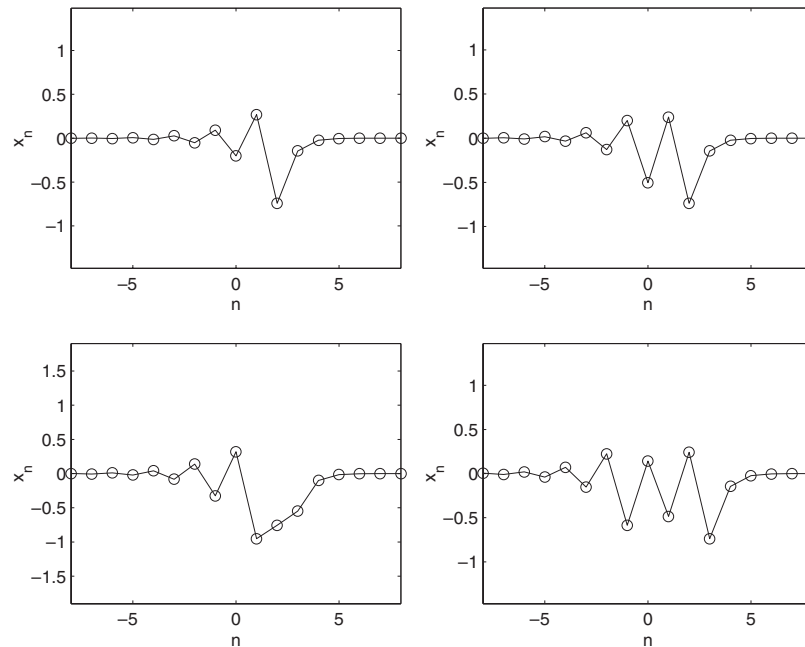


Figure 6. Several homoclinic orbits of the Hénon map (26) for $a = 1.4$ and $b = 0.3$.

topological degree method we have employed is relatively fast and very accurate. Furthermore, it is guaranteed to find all the zeros, which means that we can find all the homoclinic orbits.

The main idea of our approach is the following: given a g -dimensional invertible map, we use its inverse to embed it in a higher dimensional mapping, whose homoclinic orbits are the same as those of the original problem and are obtained as the roots of a system of nonlinear equations.

Our first method also provides a way to name all orbits using symbolic dynamics and is straightforward and easy to apply. Even though the homoclinic tangle contains an infinite number of homoclinic orbits, they can all be uniquely identified via the HOM introduced in this paper.

The HOM can also be used in another way to generate homoclinic orbits rapidly, albeit with less control over the accuracy. Starting from the trivial homoclinic orbit (i.e. all elements at the origin) and applying this map we create (at most) $k_1 \times k_2$ new approximate homoclinic orbits. When these new orbits are used as a starting point for a Newton–Raphson search (i.e. applying the method of Beyn and Kleinkauf [16, 17] with our approximate homoclinic orbit as an initial condition), we get accurate homoclinic orbits. The HOM can again be applied to each of them to get approximate homoclinic orbits and then, using a Newton–Raphson search, a large number of homoclinic orbits are generated in a very fast manner. The drawbacks of this method are: (a) the successful application of the homoclinic orbit map requires that the part of its range reached by homoclinic orbits be a subset of its domain (see section 3) and (b) the convergence of the Newton–Raphson method is not easily controlled and so the method may converge to a homoclinic orbit far from the approximated one.

The methods presented here can also easily be applied to find heteroclinic orbits. By adding and subtracting a heteroclinic orbit and its inverse, we get a new heteroclinic orbit with a well-defined symmetry. Therefore, one can again set up a system of equations whose zeros correspond to the heteroclinic orbits, following the first method. The second method can be

applied exactly as presented here. The fixed point of the constructed map now has components from both points to which the orbit is heteroclinic.

Acknowledgments

We thank S A van Gils and J C Ross for helpful discussions. This work was supported by a PENED 99-146 grant of GSRT of the Greek Ministry of Development and the ‘Karatheodory’ program of the University of Patras. Part of this work was done while JMB was a guest at the Marie Curie Training site of the Université Libre de Bruxelles.

Appendix A. Verifying the symmetry condition (7)

In this appendix we prove that, in order for equation (7) to hold for all n , it is only necessary to check this at two points $n = 0$ and $n = 1$. This we demonstrate by induction as follows: we assume that (7) holds for A_{n-1} , A_n and then show that it also holds for A_{n+1} . To see this, note that

$$S_d = S_d^{-1}, \quad \hat{G}(S_d A_n) = \begin{pmatrix} 0 & Id_d \\ Id_d & 0 \end{pmatrix} \hat{G}(A_n) \equiv R \hat{G}(A_n),$$

and that by our assumption

$$A_{-n+1} = S_d A_{n-1}, \quad A_{-n} = S_d A_n.$$

Thus, we have, from (5),

$$\begin{aligned} A_{n+1} &= L \hat{G}(A_n) - K A_{n-1} \\ &= LR \hat{G}(A_{-n}) - K S_d A_{-n+1} \\ &= LRL^{-1}(A_{-n+1} + K A_{-n-1}) - K S_d A_{-n+1} \\ &= LRL^{-1} A_{-n+1} + LRL^{-1} K A_{-n-1} - K S_d A_{-n+1} \\ &= (LRL^{-1} - K S_d) A_{-n+1} + LRL^{-1} K A_{-n-1} \end{aligned} \tag{A1}$$

and, since

$$LRL^{-1} = K S_d = \begin{pmatrix} M & 0 \\ 0 & -M \end{pmatrix}, \quad LRL^{-1} K = S_d,$$

we have proven, from (A1),

$$A_{n+1} = S_d A_{-n-1},$$

as desired.

Appendix B. The method of the topological degree

In order to find homoclinic orbits, it is necessary to find roots of systems of nonlinear equations. To do this, we use a topological degree method which is capable of finding all roots of any (finite dimensional) system of equations, within a certain region [23–26].

Let us first define the notion of the topological degree. Suppose that the function $F_n = (f_1, \dots, f_n) : D_n \subset \mathbb{R}^n \rightarrow \mathbb{R}^n$ is defined and two times continuously differentiable in an open and bounded domain D_n of \mathbb{R}^n with boundary $b(D_n)$. Suppose further that the zeros of the system of equations

$$F_n(x_1, x_2, \dots, x_n) = 0 \tag{B1}$$

(0 denotes the origin of R^n) are not located on $b(D_n)$ and they are simple, i.e. the Jacobian determinant of F_n at these zeros is nonzero. Then the *topological degree of F_n at 0 relative to D_n* is denoted by $\deg[F_n, D_n, 0]$ and can be defined by the following sum:

$$\deg[F_n, D_n, 0] = \sum_{x \in F_n^{-1}(0) \cap D_n} \operatorname{sgn} J_{F_n}(x), \quad (\text{B2})$$

where J_{F_n} denotes the determinant of the Jacobian matrix and sgn defines the three-valued sign function.

The above definition can be generalized when F_n is only continuous. In this case, Kronecker's theorem states that the system (B1) has at least one root in D_n if $\deg[F_n, D_n, 0] \neq 0$. Also, $\deg[F_n, D_n, 0]$ can be represented by the Kronecker integral which is defined as follows (see, e.g. [29]):

$$\deg[F_n, D_n, \Theta_n] = \frac{\Gamma(n/2)}{2\pi^{n/2}} \iint_{b(D_n)} \dots \int \frac{\sum_{i=1}^n A_i dx_1 \dots dx_{i-1} dx_{i+1} \dots dx_n}{(f_1^2 + f_2^2 + \dots + f_n^2)^{n/2}}, \quad (\text{B3})$$

where A_i defines the following determinants:

$$A_i = (-1)^{n(i-1)} \begin{vmatrix} f_1 & \frac{\partial f_1}{\partial x_1} & \dots & \frac{\partial f_1}{\partial x_{i-1}} & \frac{\partial f_1}{\partial x_{i+1}} & \dots & \frac{\partial f_1}{\partial x_n} \\ f_2 & \frac{\partial f_2}{\partial x_1} & \dots & \frac{\partial f_2}{\partial x_{i-1}} & \frac{\partial f_2}{\partial x_{i+1}} & \dots & \frac{\partial f_2}{\partial x_n} \\ \vdots & \vdots & \vdots & \vdots & \vdots & \vdots & \vdots \\ f_n & \frac{\partial f_n}{\partial x_1} & \dots & \frac{\partial f_n}{\partial x_{i-1}} & \frac{\partial f_n}{\partial x_{i+1}} & \dots & \frac{\partial f_n}{\partial x_n} \end{vmatrix}. \quad (\text{B4})$$

The topological degree is equal to the number of zeros of (B1) in the area D_n with positive Jacobian minus the number of roots in D_n with negative Jacobian. In general, this is not sufficient to determine the number of zeros of a system of equations. Invoking Picard's theorem, however, gives the answer: we consider an extended system of $n + 1$ equations by adding one more equation to the first n as follows:

$$f_{n+1} = x_{n+1} J_{F_n}(x_1, x_2, \dots, x_n). \quad (\text{B5})$$

The roots of the extended function $F_{n+1} = (f_1, f_2, \dots, f_n, f_{n+1}) : D_{n+1} \subset R^{n+1} \rightarrow R^{n+1}$, where D_{n+1} is the direct product of the domain D_n with an arbitrary interval of the real x_{n+1} -axis containing the point $x_{n+1} = 0$, are equal to the roots of F_n , but now they all have positive Jacobian. Thus, the topological degree of F_{n+1} is exactly equal to the number of roots of F_n in D_n .

In the case of our system of equations (8), (9) or (24), we apply Picard's theorem and calculate the number of zeros in a given region. Using bisection methods (in small dimensions) or other rootfinding methods such as Newton's or Broyden's method, we are then able to locate *every* zero in that region, and thus find the (symmetric and asymmetric) homoclinic orbits of the original system (1). Integration can be done using standard methods like the Runge–Kutta or the Monte Carlo techniques (see, e.g. [28] for implementations).

References

- [1] Holmes P and Guckenheimer J 1983 *Nonlinear Dynamical Systems and Bifurcations of Vector Fields* (New York: Springer)
- [2] Wiggins S 1988 *Global Bifurcations and Chaos* (New York: Springer)
- [3] Wiggins S 1990 *Introduction to Applied Dynamical Systems and Chaos* (New York: Springer)
- [4] Flach S 1995 *Phys. Rev. E* **51** 1504

- [5] Flach S and Willis C R 1998 *Phys. Rep.* **295** 181
- [6] Hennig D and Tsironis G 1999 *Phys. Rep.* **307** 333
- [7] Aubry S and Kopidakis G 2000 *Proc. NATO Advanced Research Workshop 'Nonlinearity and Disorder: Theory and Applications' (Tashkent, Uzbekistan)*
- [8] James G 2001 *C. R. Acad. Sci. Paris Sér. I Math.* **332** 581
- [9] Marin J L and Aubry S 1996 *Nonlinearity* **9** 1501
- [10] MacKay R S 2000 *Physica A* **288** 174
- [11] Bountis T, Capel H W, Kollmann M, Ross J C, Bergamin J M and Van der Weele J P 2000 *Phys. Lett. A* **268** 50
- [12] Bergamin J M, Bountis T and Jung C 2000 *J. Phys. A: Math. Gen.* **33** 8059
- [13] Tsironis G P 2002 *J. Phys. A: Math. Gen.* **35** 951
- [14] Friedman M J and Doedel E J 1991 *SIAM J. Numer. Anal.* **28** 789
- [15] Farantos S 1998 *Comput. Phys. Commun.* **108** 240
- [16] Beyn W-J and Kleinkauf J-M 1997 *SIAM J. Numer. Anal.* **34** 1207
- [17] Beyn W-J and Kleinkauf J-M 1997 *Numer. Algorithms* **14** 25
- [18] Fang H P 1994 *J. Phys. A: Math. Gen.* **27** 5187
- [19] Hao B-L and Zheng W-M 1998 *Applied Symbolic Dynamics and Chaos* (Singapore: World Scientific)
- [20] Rüdigerl B and Jung C 1994 *J. Phys. A: Math. Gen.* **27** 55
- [21] Rüdigerl B and Jung C 1994 *J. Phys. A: Math. Gen.* **27** 6741
- [22] Jung C, Lipp C and Seligman T H 1999 *Ann. Phys.* **275** 151
- [23] Kavvadias D J and Vrahatis M N 1996 *SIAM J. Sci. Comput.* **17** 1232
- [24] Vrahatis M N 1998 *ACM Trans. Math. Software* **14** 312
- [25] Vrahatis M N 1998 *ACM Trans. Math. Software* **14** 330
- [26] Vrahatis M N 1995 *J. Comput. Phys.* **119** 105
- [27] Hénon M 1976 *Commun. Math. Phys.* **50** 69
- [28] Vetterling W T, Press W H, Teukolsky S A and Flannery B P 2002 *Numerical Recipes: The Art of Scientific Computing* (Cambridge: Cambridge University Press)
- [29] Alexandroff P and Hopf H 1965 *Topologie* (New York: Chelsea)